CHIN. PHYS. LETT. Vol. 37, No. 3 (2020) 036701

Production of ^{87}Rb Bose–Einstein Condensate with a Simple Evaporative Cooling Method *

Rehman Fazal[1], Jia-Zhen Li(李嘉桢)[1], Zhi-Wen Chen(陈志文)[1], Yuan Qin(秦源)[1], Ya-Yi Lin(林雅益)[1], Zuan-Xian Zhang(张钻娴)[1], Shan-Chao Zhang(张善超)[1**], Wei Huang(黄巍)[1**], Hui Yan(颜辉)[1], Shi-Liang Zhu(朱诗亮)[1,2]

[1]*Guangdong Provincial Key Laboratory of Quantum Engineering and Quantum Materials, GPETR Center for Quantum Precision Measurement and SPTE, South China Normal University, Guangzhou 510006*

[2]*National Laboratory of Solid State Microstructures, School of Physics, Nanjing University, Nanjing 210093*

(Received 17 December 2019)

A Bose–Einstein condensate with a large atom number is an important experimental platform for quantum simulation and quantum information research. An optical dipole trap is the a conventional way to hold the ultracold atoms, where an atomic cloud is evaporatively cooled down before reaching the Bose–Einstein condensate. A carefully designed trap depth controlling curve is typically required to realize the optimal evaporation cooling. We present and demonstrate a simple way to optimize the evaporation cooling in a crossed optical dipole trap. A polyline shape optical power control profile is easily obtained with our method, by which a pure Bose–Einstein condensate with atom number 1.73×10^5 *is produced. Theoretically, we numerically simulate the optimal evaporation cooling using the parameters of our apparatus based on a kinetic theory. Compared to the simulation results, our evaporation cooling shows a good performance. We believe that our simple method can be used to quickly realize evaporation cooling in optical dipole traps.*

PACS: 67.85.Hj, 37.10.−x, 64.70.fm DOI: 10.1088/0256-307X/37/3/036701

Bose–Einstein condensate (BEC) of ultracold neutral atomic gases has achieved rapid development since its first production more than two decades ago. BEC has played a significant role in research, including quantum simulation, quantum computation and quantum precise measurement.[1–9] Experimental production of a BEC typically requires a few standard cooling steps, including laser cooling and trapping, sub-Doppler cooling and then evaporation cooling. The first BEC was obtained in a magnetic trap using the rf-enforced evaporation cooling technique,[10–12] after which techniques using optical traps were developed.[13–16] Although a magnetic trap is easy to build, and has a large trap volume and trap depth, typically only one single component of atoms in a specified magnetic Zeeman state can be well trapped, which limits its application where multiple components of atoms are required, such as in experiments on synthetic gauge fields, spin-orbit coupling and topological quantum matters.[17–42]

In the past two decades, several types of trapping techniques have been developed for producing multiple-component quantum gases,[43–54] including optical dipole trap (ODT) and hybrid trap that combines a magnetic trap and an ODT. An ODT can not only confine atoms with multiple spin states but can also be built with flexible geometries and with good optical access. Forced evaporation in the ODT can be directly implemented by lowering the potential trap depth U, which is determined by the power of ODT laser beams. However, complicated techniques are typically needed to optimize the evaporation cooling to achieve a BEC with a large atom number, such as numerical methods based on kinetic theory, scaling laws, multipartite method and even machine learning method.[55–63]

In this Letter, we demonstrate a simple method to realize optimal evaporative cooling in a crossed ODT. Instead of reducing the ODT trap depth following a trial exponential decay curve, we evaporatively cool down atoms by linearly ramping down the ODT laser power step by step. In each evaporation step, the ODT laser power is first ramped down to half of the starting power of this step. Then, the duration of the evaporation step is scanned to maximize the number of atoms left at the step end. This process is repeated until the production of the BEC. In our apparatus, we eventually obtained an optimal evaporation curve consisting of 5-segment straight line, by which a cloud of ^{87}Rb BEC with an atom number 1.73×10^5 is produced. The performance of this 5-segment evaporation cooling is further verified by comparing the final atom number to the theoretically optimal number.

Our BEC apparatus mainly consists of two vacuum chambers: a low vacuum chamber and a high vacuum chamber. In the low vacuum chamber, a 2-

*Supported by the National Key Research and Development Program of China (Grant Nos. 2016YFA0301803 and 2016YFA0302800), the Key-Area Research and Development Program of GuangDong Province (Grant No. 2019B030330001), the National Natural Science Foundation of China (Grant Nos. 61378012, 91636218, 11822403, 11804104, 11804105, 61875060 and U1801661), the Natural Science Foundation of Guangdong Province (Grant Nos. 2018A030313342 and 2018A0303130066), the Key Project of Science and Technology of Guangzhou (Grant No. 201804020055).

**Corresponding authors. Email: sczhang@m.scnu.edu.cn; WeiHuang@m.scnu.edu.cn

dimensional magneto-optical trap (2D-MOT) is built to produce the pre-cooled atomic beam. Then, the atomic beam is pushed to the high vacuum chamber ($P = 10^{-9}$ Pa) by a near resonant laser beam. In the high vacuum chamber, the atomic beam is captured and further cooled down by a 3-dimensional MOT (3D-MOT). These two chambers are connected by a differential pumping tube. The crossed ODT is formed by two focused Gaussian beams crossed with an angle of 90°, as shown in Fig. 1. The center of the ODT is aligned at the center of the high vacuum chamber. One ODT beam has a beam waist radius of 90 μm and initial power of 6.7 W, and is named the shallow optical dipole trap beam (SODT). The other beam has a waist radius of 60 μm and initial power of 5.3 W, and is named as the tight optical dipole trap beam (TODT). Both the ODT laser beams are generated from a single frequency and single spatial mode erbium fiber laser with wavelength 1064 nm (YFL-SF-1064 nm). The two laser beams are linearly polarized with a perpendicular polarization plane to avoid interference.

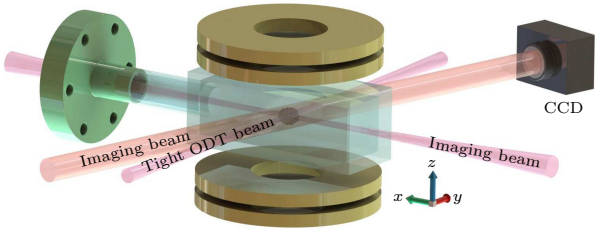

Fig. 1. A schematic diagram of the apparatus for evaporation of rubidium atoms in a crossed-beam dipole trap. The magnetic field coils are shown in brown, optical dipole trapping beams are shown in pink. The shallow ODT beam is along the x axis, while the tight ODT beam is along the y axis. An imaging beam in red is aligned with a small angle respect to the tight ODT beam. The gravity is along $-z$ direction.

An atom vapor of ^{87}Rb at room temperature is first released from a dispenser mounted in the 2D-MOT chamber. With the optimized 2D MOT and a push beam, about 3.3×10^8 atoms are loaded in the 3D MOT with a loading time of 25 s. The cooling beam of 3D MOT is red detuned by 18 MHz from the cycling transition between $|5P_{3/2}, F = 3\rangle$ and $|5S_{1/2}, F = 2\rangle$. The average intensity of three retro-reflected cooling beams is 7.8 mW/cm^2. A repump beam with the same beam size shares the same optical path of cooling beam. The average intensity of repump beam is set as 0.2 mW/cm^2. The gradient magnetic field of 3D MOT is 13 Gs/cm during atom loading in the 3D MOT, which is provided by a pair of anti-Helmholtz coils, as shown in Fig. 1. The atomic cloud in the 3D MOT is compressed by simultaneously ramping the gradient magnetic field to 39 Gs/cm and the detuning of cooling beam to 25 MHz in 100 ms. Then, we further cool down atoms to 60 μK with polarization gradient cooling by switching off the magnetic field and sweeping the cooling beam detuning to −70 MHz.

Before being transferred into the ODT, the atoms are loaded into a magnetic trap with a starting magnetic field gradient 60 Gs/cm linearly raised to 179 Gs/cm in 300 ms, during which the cooling beam and the repump beam are shut off and both the ODT lasers are switched on. With 7 s rf-enforced evaporation cooling in the magnetic trap, the atoms are finally loaded in the ODT and ready for the final evaporation cooling. With a 15 ms flat evaporative cooling, the atoms loaded in the ODT is 2.97×10^6 with temperature of 7.4 μK.

The evaporation cooling of atoms in the ODT is optimized in a simple way. We linearly ramp down the power of the ODT laser beams and separate the whole evaporation cooling into several steps. Before conducting the evaporation cooling, the lifetime of atoms in the crossed ODT is measured as T_0. With an initial ODT laser power of P_0, we perform the first step evaporation by ramping down the ODT laser power to $P_1 = P_0/2$ with trial ramping duration t_1 being $T_0/2$. By fixing the end ODT laser power as P_1, we then scan the step duration t_1 around $T_0/2$ to maximize the number of atoms left in the ODT at the end of this evaporation step. In the next evaporation step, we further linearly ramp down the ODT laser power from P_1 to $P_2 = P_1/2$ with a trial step duration t_2 of $t_1/2$, and we then scan the step duration t_2 to maximize the atom number after this step. We repeat this process until the occurrence of BEC.

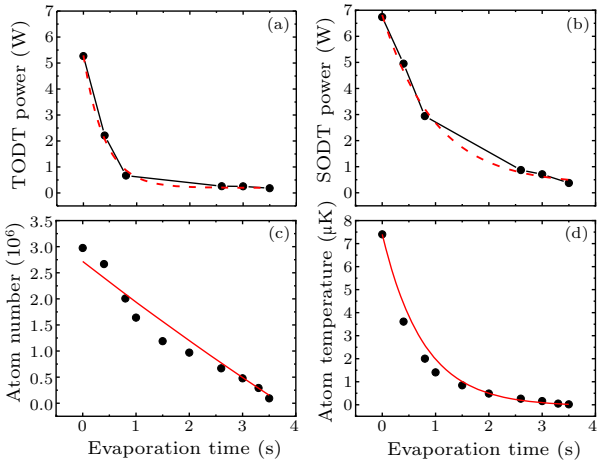

Fig. 2. The TODT (a) and SODT (b) beam power change with the evaporation time, respectively. The dark solid line is the one obtained using our optimization method. The red dashed line shows an fitted exponential decay curve as an eye-guide line. (c) The number of atoms left in the ODTs as a function of evaporation time. (d) The temperature of atoms in the ODT as a function of evaporation time.

Given that we have two laser beams making the crossed ODT, the optimization procedures are conducted one by one for both TODT and SODT iteratively. As shown in Fig. 2, we can achieve BEC with only five steps of linear evaporation. Figure 2(a) and 2(b) show the optimized polylines of TODT power and SODT power in our experiment, respectively.

Theoretically, the optimal evaporation cooling curve is an exponential decay function,[15,60,64,65] we thus plot an exponential decay curve as eye-guide line in red-dashed line that is obtained by fitting $\{(P_n, t_n), (\mathrm{n}=(0,\ldots,5)\}$ with $t_0 = 0$. Although the 5-segment polylines deviate from the exponential curve, the quickly obtained evaporation curve experimentally performs well in our apparatus.

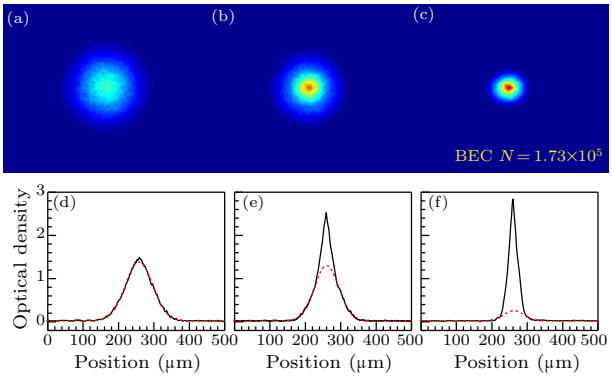

Fig. 3. Absorption images of atomic cloud with 35 ms time-of-flight at different evaporation times. (a)–(c) Phase transition of atomic cloud from thermal atoms to BEC. (d)–(f) Atomic density along the cross line through the atomic cloud center in (a)–(c), respectively. The red-dashed lines represent the fitting of thermal atoms with Gaussian function. The black-solid lines represent the fitting of atoms in the BEC state with a bimodal distribution function. The produced BEC has an atom number of 1.73×10^5.

To characterize evaporation cooling in our apparatus, we also measure the atom number and atom temperature as functions of the evaporation time, as shown in Figs. 2(c) and 2(d). When the evaporation time is 2.6 s, the SODT power is reduced to 0.87 W and the TODT power to 0.26 W, the 6.7×10^5 atoms are left in the trap with temperature of 246 nK. By reducing the SODT power to 0.527 W and TODT power to 0.192 W, part of the atoms are in the BEC state with atom number 2.91×10^5 and temperature of 49.5 nK. By further decreasing the SODT power to 0.376 W and TODT power to 0.180 W, a pure BEC with atom number of 1.73×10^5 and temperature of 17 nK is achieved. The phase transition procedure of atoms in thermal gas state to the pure BEC state is shown in Figs. 3(a)–3(c) by measuring the time-of-flight absorption images of the atomic cloud at the above three instants. Figures 3(d)–3(f) show the fitting of the atomic density along the cross line through the atomic cloud center in Figs. 3(a)–3(c). The Gaussian shape atomic density that tells us the pure thermal atomic gas is gradually changed into an atomic density with bimodal distribution that verifies the production of pure BEC during the evaporation curve.

The efficiency of our evaporative cooling is compared to the theoretically optimal value predicted by a kinetic model reported in Ref. [43] using the parameters in our apparatus. This kinetic model describes the time-dependent variation of the atom number and temperature in a crossed ODT during evaporation cooling. With this model, the evolution equations of average atom energy and number in a deep 3D harmonic traps take the following forms by accounting for the elastic collision rate change, one body and three-body losses and the trap geometry change:

$$\dot{E} = -N\Gamma_{\mathrm{ev}}(\eta+\kappa)k_{\mathrm{B}}T + vE\frac{\dot{T}}{T} - \Gamma_{1\mathrm{B}}E - \Gamma_{3\mathrm{B}}\frac{2}{3}E, \quad (1)$$

$$\dot{N} = -\left(\Gamma_{\mathrm{ev}} + \Gamma_{1\mathrm{B}} + \Gamma_{3\mathrm{B}}\right)N, \quad (2)$$

where three-body loss rate $\Gamma_{3\mathrm{B}} = L_{3\mathrm{B}}n_0^2/(3\sqrt{3})$ with $L_{3\mathrm{B}} = 4.3(\pm1.8) \times 10^{-29}\mathrm{cm}^6/\mathrm{s}$ for Rb^{87} in the $F = 1$ ground state.[66] $\Gamma_{1\mathrm{B}} = 1/21s^{-1}$ is one-body loss rate determined by background collisions, which is measured by the atom lifetime in the ODT. The evaporation rate is well approximated by $\Gamma_{\mathrm{ev}} \approx (\eta - 4)e^{-\eta}\Gamma_{\mathrm{el}}$.[55,59] Here, Γ_{el} is the elastic collision rate in a 3D harmonic trap $\Gamma_{\mathrm{el}} = n\sigma\bar{v}/(2\sqrt{2})$, where $\sigma = 8\pi a_{\mathrm{s}}^2$ is the elastic cross section and a_{s} is the s-wave scattering length. Rb^{87} has $a_{\mathrm{s}} = 98a_0$ with a_0 as the Bohr radius.[67] The average velocity of atoms is $\bar{v} = 4\left(k_{\mathrm{B}}T/\pi m\right)^{1/2}$ and average energy removed by each evaporated atom is $(\eta+\kappa)k_{\mathrm{B}}T$, where $\kappa \approx (\eta-5)/(\eta-4)$.

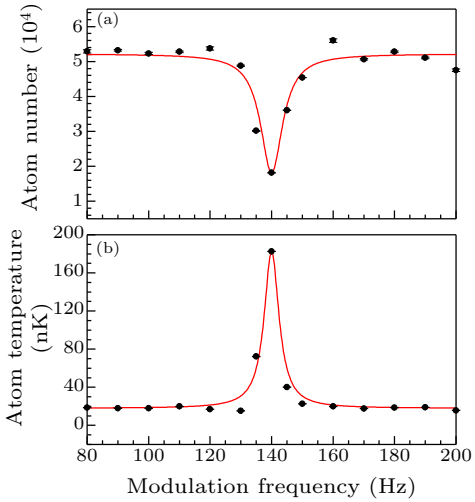

Fig. 4. Measurement of the trap frequency by parametric heating of atomic cloud. We scan the modulation frequency and measure the atom number and temperature. Lorentz fitting is used to extract the peak position as shown by the red-solid line. A dip of the atom number means that the modulation frequency is twice the ODT trap frequency. A peak appearing in the atom temperature spectrum confirms the measured trap frequency.

Besides these parameters, two more parameters—η and ν—are also required to numerically solve the kinetic Eq. (1). Here, ν is determined from the relationship between the average trap frequency $\bar{\omega}$ and the trap depth U with formula $\bar{\omega} \propto U^{\nu}$; $\eta = U/k_{\mathrm{B}}T$ is the ratio of trap depth U to atom cloud temperature T, where k_{B} is Boltzmann's constant. To determine η and ν, average trap frequency $\bar{\omega} = (\omega_x\omega_y\omega_z)^{1/3}$ and trap depth U are experimentally measured. The

conventional parametric heating technique is used to measure the trap frequency of the crossed ODT. The TODT laser power is modulated with an amplitude of 5% and duration of 0.5 s. With a modulation frequency that is twice the trap frequencies, atoms would be quickly heated up and lost away from the ODT. The atom loss dip and temperature peak are observed at the same modulation frequency, which also verify our measurements, as shown in Figs. 4(a) and 4(b).

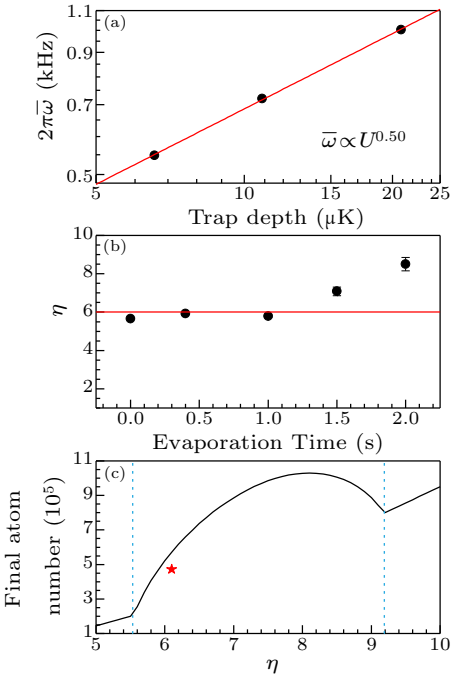

Fig. 5. (a) Measured average trap frequency $\bar{\omega}$ and calibrated trap depth U are used to fit out the $\nu = 0.50$. (b) Extracted η during evaporation based on the temperature of atoms measured and calibrated trap depth U. (c) Numerically computed final atom number $N_{\rm f}$ when reaching the phase-space density $\rho_{\rm f} = 2.6$ as a function of η. The initial parameters are $T = 7.4\,\mu$K, $N = 2.97 \times 10^6$, $\bar{\omega} = 2\pi \times 220\,$Hz, $\Gamma_{\rm IB} = 1/21\,{\rm s}^{-1}$. Since $N_{\rm i}$, $\rho_{\rm i}$ and $\rho_{\rm f}$ are fixed, $\gamma_{\rm eff}$ depends only on $N_{\rm f}$. The numerical calculated maximum final atom number is achieved at $\eta = 8.1$. In our experiment the η is about 6.1, marked with a red star. The η value in the area between the two blue-dashed lines can reach BEC.

Figure 5(a) shows the dependence of measured average trap frequency $\bar{\omega}$ on the calibrated trap depth U, from which $\nu = 0.50$ is extracted using linear fitting. Here η is obtained using the measured atom temperature and calibrated trap depth U, as shown in Fig. 5(b). Initially, η is almost a constant value of 6.1 with small fluctuation due to the errors in the atom temperature measurements. By substituting the above measured parameters of our ODT that initially $T = 7.4\,\mu$K, $N = 2.97 \times 10^6$, $\bar{\omega} = 2\pi \times 220\,$Hz, the optimal final atom number $N_{\rm f}$ after evaporation cooling is solved by assuming the final phase-space density to be $\rho_{\rm f} = 2.6$. With a fixed starting phase space density, the evaporation efficiency only depends on $N_{\rm f}$. In our apparatus, the geometry of the crossed ODT is unchanged during evaporation and thus a constant $\nu = 0.50$ is used in the numerical calculations. The final atom number after evaporation cooling, $N_{\rm f}$, as a function of η is plotted in Fig. 5(c). The dark-solid line represents the numerical results and the red star represents the measured atom number of 4.71×10^5 during the evaporation cooling when BEC is observed. With $\eta = 6.1$ during the evaporation cooling, the theoretically optimal final atom number $N_{\rm f}$ is 5.72×10^5, which verifies that the 5-segment evaporation curve performs well and efficiently. The two blue-dashed vertical lines in Fig. 5(c) mark out the area that the BEC can be realized with $5.5 < \eta < 9.2$.

In summary, we have reported and demonstrated a simple method to optimize the evaporation cooling of atoms in an ODT. By linearly ramping down the ODT laser power, we have designed an evaporation control curve consisting of five segments in a linear control curve. With this simple method, we have achieved a pure BEC with an atom number of 1.73×10^5. The evaporation cooling performance of our linear ramping curve is further verified by comparing it to that of the theoretically optimal evaporation cooling. Compared to the conventional optimization method, our method of optimizing the evaporation cooling in the ODT is easy to implement experimentally, even without detailed knowledge of an ODT.

References

[1] Grenier M, Mandel O, Esslinger T, Hänsch T W and Bloch I 2002 *Nature* **415** 39
[2] Léonard J, Morales A, Zupancic P, Esslinger T and Donner T 2017 *Nature* **543** 87
[3] Léonard J, Morales A, Zupancic P, Donner T and Esslinger T 2017 *Science* **358** 1415
[4] Steinke S K, Singh S, Tasgin M E, Meystre P, Schwab K C and Vengalattore M 2011 *Phys. Rev. A* **84** 023841
[5] Calarco T, Dorner U, Julienne P S, Williams C J and Zoller P 2004 *Phys. Rev. A* **70** 012306
[6] Byrnes T, Wen K and Yamamoto Y 2012 *Phys. Rev. A* **85** 040306(R)
[7] Vinit A and Raman C 2017 *Phys. Rev. A* **95** 011603
[8] Rudolph J, Herr W, Grzeschik C, Sternke T, Grote A, Popp M, Becker D, Mntinga H, Ahlers H, Peters A, Lmmerzahl C, Sengstock K, Gaaloul N, Ertmer W and Rasel E M 2015 *New J. Phys.* **17** 065001
[9] Pyrkov A N and Byrnes T 2013 *New J. Phys.* **15** 093019
[10] Ketterle W and Van D N J 1996 *Adv. At. Mol. Opt. Phys.* **37** 181
[11] Mewes M O, Andrews M R, Druten N J V, Kurn D M, Durfee D S, Townsend C G and Ketterle W 1996 *Phys. Rev. Lett.* **77** 988
[12] Jin D S, Ensher J R, Matthews M R, Wieman C E and Cornell E A 1996 *Phys. Rev. Lett.* **77** 420
[13] Urvoy A, Vendeiro Z, Ramette J, Adiyatullin A and Vuletić V 2019 *Phys. Rev. Lett.* **122** 203202
[14] Colzi G, Fava E, Barbiero M, Mordini C, Lamporesi G and Ferrari G 2018 *Phys. Rev. A* **97** 053625
[15] Xie D Z, Wang D Y, Gou W, Bu W H and Yan B 2018 *J. Opt. Soc. Am. B* **35** 500
[16] Jacob D, Mimoun E, Sarlo L D, Weitz M, Dalibard J and Gerbier F 2011 *New J. Phys.* **13** 065022
[17] Zhang D W, Zhu Y Q, Zhao Y X, Yan H and Zhu S L 2018 *Adv. Phys.* **67** 253
[18] Lin Y J, Jiménez G K and Spielman I B 2011 *Nature* **471** 83

[19] Williams R A, LeBlanc L J, Jiménez G K, Beeler M C, Perry A R, Phillips W D and Spielman I B 2012 *Science* **335** 314
[20] Ji S C, Zhang J Y, Zhang L, Du Z D, Zheng W, Deng Y J, Zhai H, Chen S and Pan J W 2014 *Nat. Phys.* **10** 314
[21] Wu X, Zhang L, Sun W, Xu T X, Wang Z B, Ji C S, Deng J Y, Chen S, Liu J X and Pan J W 2016 *Science* **354** 83
[22] Clark L M, Feng L and Chin C 2016 *Science* **354** 606
[23] Sugawa S J, Salces C F, Perry A R, Yue Y C and Spielman I B 2018 *Science* **360** 1429
[24] Deng S J, Shi Z Y, Diao P P, Yu Q L, Zhai H, Qi R and Wu H B 2016 *Science* **353** 371
[25] Tang P J, Peng P, Li Z H, Chen X Z, Li X P and Zhou X J 2019 *Phys. Rev. A* **100** 013618
[26] Luo X Y, Zou Y Q, Wu L N, Liu Q, Han M F, Tey M K and You L 2017 *Science* **355** 620
[27] Chen L C, Wang P J, Meng Z M, Huang L H, Cai H, Wang D W, Zhu S Y and Zhang J 2018 *Phys. Rev. Lett.* **120** 193601
[28] Hu Z F, Liu C P, Liu J M and Wang Y Z 2018 *Opt. Express* **26** 20122
[29] Zhang D F, Gao T Y, Zou P, Kong L R, Li R Z, Shen X, Chen X L, Peng S G, Zhan M S, Pu H and Jiang K J 2019 *Phys. Rev. Lett.* **122** 110402
[30] Deng L, Hagley E W, Cao Q, Wang X R, Luo X Y, Wang R Q, Payne M G, Yang F, Zhou X J, Chen X Z and Zhan M S 2010 *Phys. Rev. Lett.* **105** 220404
[31] Dai H N, Yang B, Reingruber A, Xu X F, Jiang X, Chen Y A, Yuan Z S and Pan J W 2016 *Nat. Phys.* **12** 783
[32] Yang B, Chen Y Y, Zheng Y G, Sun H, Dai H N, Guan X W, Yuan Z S and Pan J W 2017 *Phys. Rev. Lett.* **119** 165701
[33] Yang S F, Xu Z T, Wang K, Li X F, Zhai Y Y and Chen X Z 2019 *Chin. Phys. Lett.* **36** 080302
[34] Nawaz K S, Mi C D, Chen L C, Wang P J and Zhang J 2019 *Chin. Phys. Lett.* **36** 043201
[35] Qi W, Liang M C, Zhang H, Wei Y D, Wang W W, Wang X J and Zhang X B 2019 *Chin. Phys. Lett.* **36** 093701
[36] Peng P, Huang L H, Li D H, Wang P J, Meng Z M and Zhang J 2018 *Chin. Phys. Lett.* **35** 063201
[37] Ma X B, Ye Z X, Xie L Y, Guo Z, You L and Tey M K 2019 *Chin. Phys. Lett.* **36** 073401
[38] Zhou J W, Li X X, Gao R, Qin W S, Jiang H H, Li T T and Xue J K 2019 *Chin. Phys. Lett.* **36** 090302
[39] Wei Y W, Kong C and Hai W H 2019 *Chin. Phys. B* **28** 056701
[40] Huang L H, Wang P J, Fu Z K and Zhang J 2014 *Chin. Phys. B* **23** 013402
[41] Liu C, Yang Z Y, Zhao L C, Yang W L and Yue R H 2013 *Chin. Phys. Lett.* **30** 040304
[42] Wang Y M and Liang J Q 2012 *Chin. Phys. B* **21** 060305
[43] Olson A J, Niffenegger R J and Chen Y P 2013 *Phys. Rev. A* **87** 053613
[44] Kinoshita T, Wenger T and Weiss D S 2005 *Phys. Rev. A* **71** 011602
[45] Lin Y J, Perry A R, Compton R L, Spielman I B and Porto J V 2009 *Phys. Rev. A* **79** 063631
[46] Roy R, Green A, Bowler R and Gupta S 2016 *Phys. Rev. A* **93** 043403
[47] Dunning A, Gregory R, Bateman J, Himsworth M and Freegarde T 2015 *Phys. Rev. Lett.* **115** 073004
[48] Schemmer M and Bouchoule I 2018 *Phys. Rev. Lett.* **121** 200401
[49] Hu J, Urvoy A, Vendeiro Z, Crépel V, Chen W and Vuletić V 2017 *Science* **358** 1078
[50] Jiang J, Zhao L, Webb M, Jiang N, Yang H and Liu Y 2013 *Phys. Rev. A* **88** 033620
[51] Song B, He C D, Zhang S C, Hajiyev E, Huang W, Liu X J and Jo G B 2016 *Phys. Rev. A* **94** 061604(R)
[52] Granade S R, Gehm M E, O'Hara K M and Thomas J E 2002 *Phys. Rev. Lett.* **88** 120405
[53] Hansen A H, Khramov A Y, Dowd W H, Jamison A O, Plotkin S B, Roy R J and Gupta S 2013 *Phys. Rev. A* **87** 013615
[54] Duan Y F, Jiang B N, Sun J F, Liu K K, Xu Z and Wang Y Z 2013 *Chin. Phys. B* **22** 056701
[55] Hung C L, Zhang X, Gemelke N and Chin C 2008 *Phys. Rev. A* **78** 011604
[56] Clément J F, Brantut J P, Robert S V M, Nyman R A, Aspect A, Bourdel T and Bouyer P 2009 *Phys. Rev. A* **79** 061406
[57] Arnold K and Barrett M 2011 *Opt. Commun.* **284** 3288
[58] Weber T, Herbig J, Mark M, Nägerl H C and Grimm R 2003 *Science* **299** 232
[59] Luiten O J, Reynolds M W and Walraven J T M 1996 *Phys. Rev. A* **53** 381
[60] O'Hara K M, Gehm M E, Granade S R and Thomas J E 2001 *Phys. Rev. A* **64** 051403(R)
[61] Williams M J and Fertig C 2015 *Phys. Rev. A* **91** 023432
[62] Yamashita M, Koashi M, Mukai T, Mitsunaga M, Imoto N and Mukai T 2003 *Phys. Rev. A* **67** 023601
[63] Wigley P B, Everitt P J, Hengel A V D, Bastian J W, Sooriyabandara M A, McDonald G D, Hardman K S, Quinlivan C D, Manju P, Kuhn C N N, Petersen I R, Luiten A N, Hope J J, Robins N P and Hush M R 2016 *Sci. Rep.* **6** 25890
[64] Stellmer S, Tey M K, Huang B, Grimm R and Schreck F 2009 *Phys. Rev. Lett.* **103** 200401
[65] Mishra H P, Flores A S, Vassen W and Knoop S 2015 *Eur. Phys. J. D* **69** 52
[66] Burt E A, Ghrist R W, Myatt C J, Holland M J, Cornell E A and Wieman C E 1997 *Phys. Rev. Lett.* **79** 337
[67] Kempen E G M V, Kokkelmans S J J M F, Heinzen D J and Verhaar B J 2002 *Phys. Rev. Lett.* **88** 093201